Laser Physics, Vol. 15, No. 2, 2005, pp. 395–400.

Vortex States in Fermi–Bose Mixtures

M. Guilleumas[1, *], D. M. Jezek[2], M. Barranco[1], R. Mayol[1], and M. Pi[1]

[1] *Departament d'Estructura i Constituents de la Matèria, Facultat de Física, Universitat de Barcelona, E-08028 Barcelona, Spain*

*e-mail: muntsa@ecm.ub.es

[2] *Departamento de Física, Facultad de Ciencias Exactas y Naturales, Universidad de Buenos Aires, RA-1428 Buenos Aires, and Consejo Nacional de Investigaciones Científicas y Técnicas, Argentina*

Received July 14, 2004

Abstract—We consider a vortex state in a confined mixture of bosons and fermions in the quantal degeneracy regime with attractive boson–fermion interactions. Within a mean-field description, we obtain the equilibrium configurations and investigate the phase-stability diagram of the K–Rb mixture assuming that the Bose–Einstein condensate sustains a quantized vortex line.

The study of quantum degenerate atomic Bose–Fermi mixtures has become very active in the field of dilute quantum gases. Degenerate Bose–Fermi mixtures are very rich systems: depending on the relative sign and magnitude of the scattering lengths, the mixture can coexist, phase-separate, or collapse [1, 2]. In particular, Bose–Fermi mixtures in which the fermions are well inside the boson cloud are very appealing, since this implies an efficient sympathetic cooling of the fermionic species down to the degenerate regime and opens the possibility of investigating the BCS transition of Cooper pairs.

So far the mixtures experimentally realized are the following three: ^{6}Li–^{7}Li [3], ^{6}Li–^{23}Na [4], and ^{40}K–^{87}Rb [2, 5, 6]. The first two mixtures are characterized by a repulsive Fermi–Bose interaction and, therefore, do not exhibit a large overlap between the two species, but they could undergo a two-component separation [2, 5]. On the contrary, ^{40}K–^{87}Rb mixtures have a large attractive boson–fermion interaction, thus allowing for an overlap between fermions and bosons. This mixture was first obtained by the LENS group, who observed the collapse above some critical values of the particle numbers [7] and determined the interspecies scattering length from collisional measurements [6, 8, 9]. Very recently a new experimental determination of the boson–fermion interaction of the ^{40}K–^{87}Rb mixture was done in JILA by measuring the relaxation rates [10]; the value obtained is in slight disagreement with the one obtained in [6, 8].

From a theoretical point of view, a fairly large amount of work has been devoted to the study of boson-fermion mixtures, including their ground-state configurations [1, 2, 11] and the spectrum of collective excitations [12, 13], but the study of vortex states has not been yet addressed in degenerate Bose–Fermi mixtures, only in binary Bose–Bose mixtures [14]. The occurrence of quantized vortices is an essential feature of superfluid systems [15]. Since their first experimental observation [16], these topological singularities have been studied in detail in confined condensates (see [17–19] and references therein). It may thus be interesting to investigate the physical appearance of such vortices that arise in the bosonic component in the presence of a fermionic cloud that is in the normal (nonsuperfluid), but quantum degenerate, phase. This is the aim of our work, which bears some similarities with the description of quantized vortices in ^{3}He–^{4}He nanodroplets that was recently addressed [20].

This work is organized as follows. In Section 1, we describe the mean-field model we used. In Section 2, we derive analytical expressions for the position of the maximum of the bosonic and fermionic densities in some particular cases. In Section 3, we present the numerical results obtained by solving the mean-field coupled equations when the condensate sustains a quantized vortex for a different number of bosons and fermions up to the critical values where collapse of the mixture occurs. A summary is given in Section 4.

1. THE MEAN-FIELD MODEL

We consider a mixture of a Bose–Einstein condensate (B) and a degenerate Fermi gas (F) at zero temperature confined in spherically symmetric traps V_B and V_F and with angular frequencies ω_B, ω_F for bosons and fermions, respectively.

Within the mean-field framework, bosons are described by the Gross–Pitaevskii theory and, for the fermionic component, the Thomas–Fermi–Weizsäcker (TFW) approximation provides a good description when the number of trapped fermions is large [2]. The fermionic kinetic-energy density can then be written as a function of the local fermion density n_F and its gradients. For fully polarized spin-1/2 fermions, it reads

$$\tau_F(\vec{r}) = \frac{3}{5}(6\pi^2)^{2/3} n_F^{5/3} + \beta\frac{(\nabla n_F)^2}{n_F}, \qquad (1)$$

where M_F is the mass of the fermionic species. The Weizsäcker coefficient β is fixed at 1/18. This term contributes little to the kinetic energy, and it is usually neglected [2]. However, its inclusion [13] has the major advantage that it yields an Euler–Lagrange (EL) equation for n_F that is well-behaved everywhere, thus avoiding the classical turning-point problem that arises when this term is neglected (the Thomas–Fermi approximation).

Neglecting all *p*-wave interactions, the energy-density functional for the Bose–Fermi mixture at zero temperature has the form [2]

$$\mathscr{E}(\vec{r}) = \frac{\hbar^2}{2M_B}|\nabla\Psi|^2 + V_B n_B + \frac{1}{2}g_{BB}n_B^2 + g_{BF}n_F n_B + \frac{\hbar^2}{2M_F}\tau_F + V_F n_F, \quad (2)$$

where $n_B = |\Psi|^2$ is the condensate density and M_B is the boson atomic mass. The boson–boson and boson–fermion coupling constants g_{BB} and g_{BF} are written in terms of the *s*-wave scattering lengths a_B and a_{BF} as $g_{BB} = 4\pi a_B\hbar^2/M_B$ and $g_{BF} = 4\pi a_{BF}\hbar^2/M_{BF}$, respectively. We have defined $M_{BF} \equiv 2M_B M_F/(M_B + M_F)$.

When the condensate sustains a quantized vortex line along the z axis, the condensate wave function can be written using the Feymann–Onsager ansatz as $\Psi = |\Psi|e^{im\phi}$, where $m = 1, 2, 3\ldots$ is the circulation quantum number and ϕ is the angle around the z axis. The kinetic-energy density for the bosonic component is then

$$\frac{\hbar^2}{2M_B}|\nabla\Psi|^2 = \frac{\hbar^2}{2M_B}(\nabla|\Psi|)^2 + \frac{\hbar^2 m^2}{2M_B}\frac{n_B}{r^2}. \quad (3)$$

The second term is the centrifugal energy arising from the velocity flow of bosons around the vortex core with quantized circulation, which pushes the bosonic atoms away from the core. In the present paper, we have considered only singly quantized vortices ($m = 1$). We assume that the Fermi component is not superfluid and consider it to be in a stationary state. This situation can be achieved experimentally by waiting sufficiently long after the generation of the vortex in the condensate for the drag force between bosons and fermions to dissipate.

The variation of $\mathscr{E}$ with respect to Ψ and n_F, under the constraint of the given number of bosons and fermions (N_B and N_F), yields the following coupled Euler–Lagrange equations:

$$\left(-\frac{\hbar^2\nabla^2}{2M_B} + V_B + \frac{\hbar^2 m^2}{2M_B}\frac{1}{r^2} + g_{BB}n_B + g_{BF}n_F\right)\Psi = \mu_B\Psi, \quad (4)$$

$$\frac{\hbar^2}{2M_F}\left[(6\pi^2)^{2/3}n_F^{5/3} + \beta\frac{(\nabla n_F)^2}{n_F} - 2\beta\Delta n_F\right] + V_F n_F + g_{BF}n_B n_F = \mu_F n_F, \quad (5)$$

where μ_B and μ_F are the boson and fermion chemical potentials, respectively. Eq. (4) is the Gross–Pitaevskii (GP) equation for bosons with a new term describing the boson–fermion interaction. The ground state ($m = 0$) or a vortical state can be obtained by solving the GP equation for bosons (Eq. (4)) coupled to the Thomas–Fermi–Weizsäcker equation for fermions (Eq. (5)). Due to the inclusion of the Weizsäcker term in $\mathscr{E}(\vec{r})$, solving Eq. (5) is no more complicated than solving the GP equation. This can be readily seen by writing the latter in terms of n_B:

$$\frac{\hbar^2}{2M_B}\left[\frac{1}{4}\frac{(\nabla n_B)^2}{n_B} - \frac{1}{2}\Delta n_B\right] + V_B n_B + \frac{\hbar^2 m^2}{2M_B}\frac{n_B}{r^2} + g_{BB}n_B^2 + g_{BF}n_B n_F = \mu_B n_B, \quad (6)$$

which is formally equivalent to Eq. (5). We have discretized these equations using nine-point formulas and have solved them on a 2D (r, z) mesh. The results have been tested for different sizes of the spatial steps ($\Delta r = \Delta z \sim 0.1$ μm). We have employed the imaginary time method to find the solution of these coupled equations written as imaginary time diffusion equations [21]. After every imaginary time step, the densities are normalized to the corresponding particle numbers. To start the iteration procedure, we used positive random numbers to build both normalized densities. This avoids the introduction of any bias in the final results. We also checked that the solutions fulfill the generalized virial theorem [22].

2. DENSITY PROFILES: ANALYTICAL CONSIDERATIONS

We investigate the shape of the density profiles and obtain analytical expressions for the position of the maximum of the bosonic and fermionic density in two limiting cases. These points are interesting since it is around them that the densities grow indefinitely and, thus, the mixture collapses. In the next section, we will see that these analytical expressions obtained in two particular cases remain valid for an arbitrary number of fermions and bosons.

2.1. Large Number of Bosons

Let us consider a large Bose condensate in the Thomas–Fermi (TF) regime and a small number of fermions. The condensate density hosting a vortex line along the z axis can be approximated from Eq. (4) by neglecting the first kinetic energy term and the interaction term with fermions [17]:

$$n_B^v = \frac{1}{g_{BB}}\left[\mu_B - \frac{\hbar^2 m^2}{2M_B}\frac{1}{r^2} - V_B\right] \times \Theta\left[\mu_B - \frac{\hbar^2 m^2}{2M_B}\frac{1}{r^2} - V_B\right], \tag{7}$$

with $\Theta(x) = 1$ if $x > 0$ and zero otherwise. This density is zero at $r = 0$ due to the flow around the vortex core and reaches its maximum value on a circle of radius $r_0 = \sqrt{\hbar m/(M_B\omega_{rB})}$ around that axis. We consider now the effect of a quantized boson vortex line in the fermion distribution. The effective fermion potential has two main terms, namely, the external potential and the mean-field term arising from the interaction with the bosons, which is proportional to the condensate density:

$$V_v^{\text{eff}} = V_F + g_{BF}n_B^v = \frac{1}{2}M_F(\omega_{rF}^2 r^2 + \omega_{zF}^2 z^2) + g_{BF}n_B^v. \tag{8}$$

The minimum of V_v^{eff} inside the condensate can be calculated using n_B^v and defining the dimensionless parameter

$$\gamma_i \equiv 1 - \frac{a_{BF}M_B^2\omega_{iB}^2}{a_B M_{BF} M_F \omega_{iF}^2} \tag{9}$$

with $i = r, z$; this yields that it is located at $z' = 0$ and

$$r' = (1-\gamma_r^{-1})^{1/4}\sqrt{\frac{\hbar m}{M_B\omega_{rB}}} = (1-\gamma_r^{-1})^{1/4} r_0. \tag{10}$$

Thus, the minimum of the effective fermion potential and, therefore, the maximum of the fermion density is attained on a circle of radius r' around the vortex line.

2.2. Large Number of Both Bosons and Fermions

We consider now a Bose–Fermi mixture with a large number of bosons and fermions. In this case, the effect of the fermions in the GP equation cannot be neglected. However, the gradient terms in the EL equations can be neglected since both components are large; in the case of bosons, this is the TF approximation, and in the case of fermions, the gradient term is a correction to the leading term proportional to $n_F^{5/3}$. From Eq. (4) we obtain the following expression for n_B:

$$n_B = \frac{1}{g_{BB}}\left[\mu_B - V_B - \frac{\hbar^2 M^2}{2M_B}\frac{1}{r^2} - g_{BF}n_F\right]. \tag{11}$$

Substituting it into Eq. (5), where the gradient terms have been neglected, and deriving the resulting expression with respect to r, we get

$$\frac{1}{3}\frac{\hbar^2}{M_F}(6\pi^2)^{2/3}n_F^{-1/3}\frac{\partial n_F}{\partial r} - \frac{g_{BF}}{g_{BB}}M_B\omega_{rB}^2 r + M_F\omega_{rF}^2 r + \frac{\hbar^2 m^2}{M_B}\frac{1}{r^3} - \frac{g_{BF}^2}{g_{BB}}\frac{\partial n_F}{\partial r} = 0. \tag{12}$$

The extremum in the fermionic density is found by setting $\partial n_F/\partial r = 0$ with $n_F \neq 0$, which means that the following equation has to be fulfilled:

$$-\frac{g_{BF}}{g_{BB}}M_B\omega_{rB}^2 r + M_F\omega_{rF}^2 r + \frac{\hbar^2 m^2}{M_B}\frac{1}{r^3} = 0, \tag{13}$$

whose solution coincides precisely with the value of r' found in the previous case (Eq. (10)).

3. NUMERICAL RESULTS

We consider a singly quantized vortex line along the z axis in a ^{40}K–^{87}Rb mixture. We have assumed spherically symmetric traps for bosons and fermions, with the trap frequencies $\omega_B = 2\pi \times 100$ Hz and $\omega_F = \sqrt{M_B/M_F}\omega_B$. Using the set of scattering lengths of [9], namely, $a_B = 98.98a_0$ and $a_{BF} = -395a_0$, where a_0 is the Bohr radius, dimensionless parameters (9) introduced in the previous section are $\gamma_r^{-1} = 0.136$ and $(1-\gamma_r^{-1})^{1/4} = 0.964$. And using the value of the boson–fermion scattering length measured in JILA [10], $a_{BF} = -250a_0$, we find $\gamma_r^{-1} = 0.1996$ and $(1-\gamma_r^{-1})^{1/4} = 0.946$. The two values of a_{BF} yield different values of γ_r. However, from Eq. (10) it follows that, in the presence of a vortex state in ^{40}K–^{87}Rb mixtures, the position of the maximum of the fermionic density is very close to the bosonic one for the two different boson–fermion scattering lengths measured in [9] and [10]: $r' \sim 0.96r_0$.

We have numerically solved Eqs. (5) and (6) for different numbers of bosons and fermions using the set of scattering lengths from [9]. We plot in Fig. 1 several density profiles in the $z = 0$ plane for configurations hosting a singly quantized vortex line in the condensate. We have fixed $N_B = 10^5$ and have considered three different fermion numbers, namely, $N_F = 0$ (dotted line), 1500 (solid line), and 15000 (dashed line). As expected, the condensate density vanishes on the z axis due to the velocity flow of ^{87}Rb atoms around the vortex core. When $N_F = 0$, the maximum of the condensate density is located in the $z = 0$ plane, in a circle of radius $r_0 = 1.13$ μm that is marked with a vertical line in the graph. The density profiles of fermions are also peaked around r_0 independently of the number of trapped fer-

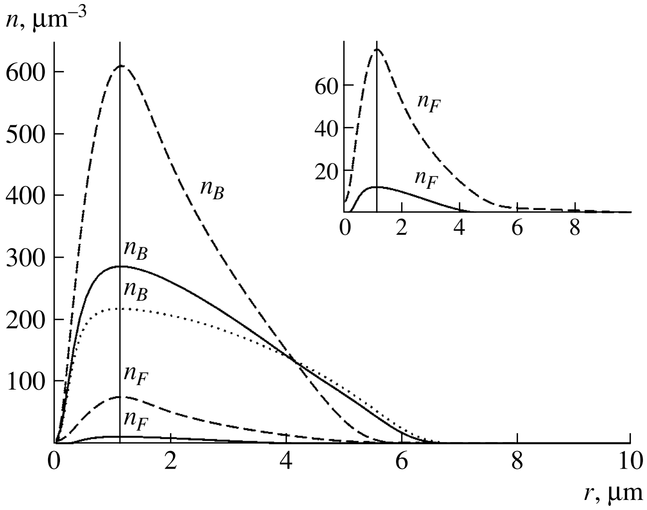

Fig. 1. Boson and fermion density profiles in the $z = 0$ plane of ^{40}K–^{87}Rb configurations hosting a vortex line with $m = 1$. In all cases, $N_B = 10^5$. The different lines correspond to $N_F = 0$ (dotted line), $N_F = 1500$ (solid lines), and $N_F = 15000$ (dashed lines). The inset shows a magnified view of the fermion density distributions.

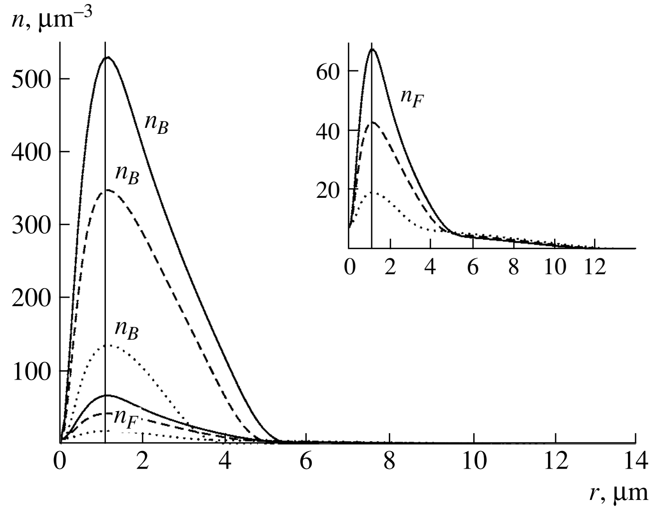

Fig. 2. Boson and fermion density profiles in the $z = 0$ plane of ^{40}K–^{87}Rb configurations hosting a vortex line with $m = 1$. In all cases, $N_F = 20000$. The different lines correspond to $N_B = 10000$ (dotted lines), $N_B = 50000$ (dashed lines), and $N_B = 80000$ (solid lines). The inset shows a magnified view of the fermion density distributions.

mions. This is in agreement with the positions $r' \sim 0.96r_0$ obtained using the simplified model of the previous section. It is interesting to note that upon increasing N_F at a constant N_B, the fermion and boson density profiles become sharper due to their mutual attraction. The attractive boson–fermion interaction produces an enhancement of the density of both species in the overlap volume.

It can be seen in Fig. 1 that fixed N_B when the fermion concentration is small, namely, $N_F/N_B \le 5\%$ (solid line), the fermion cloud is completely inside the condensate because the attractive interaction between bosons and fermions dominates the repulsion of the Pauli principle. However, when the number of trapped fermions is above a certain value, namely, $N_F/N_B \sim 10\%$, a fairly large number of fermions remains unmixed. In this case, the Pauli principle forces the fermions to occupy excited single particle states of the trapping potential with a larger radial extension, whereas the bosons are in the vortex state. The manifestation of the Fermi pressure can be seen in the inset of Fig. 1 as the long tail in the fermion density profile outside the condensate for a dilution $N_F/N_B = 15\%$ (dashed line). It is interesting to note that, when the condensate hosts a vortex line, fermions can separate from bosons not only outside the condensate but also occupying the region inside the vortex core (see the finite fermion density along the z axis).

In Fig. 2 we plot several density profiles in the $z = 0$ plane for a fixed number of fermions $N_F = 20000$, and we consider three different numbers of condensate atoms, namely, $N_B = 10000$ (dotted line), 50000 (dashed line), and 80000 (solid line), all of which host a quantized vortex line along the z axis. From this figure one can see that, even for large fermion concentrations $N_F/N_B > 25\%$, the densities of fermions are peaked around the maximum of the condensate density, which remains in the same position, namely, $r_0 = 1.13$ μm, as in the case of a vortex state in a pure condensate (marked with a vertical line in the graph). The enhancement of the overlapping densities increases with the N_B due to the attractive interaction between bosons and fermions. And the tail of fermions outside the condensate increases with N_F/N_B, as the number of fermions without mixing increases.

Due to the attractive boson–fermion interaction, stable trapped ^{40}K–^{87}Rb mixtures can only have a limited number of fermions and bosons. If the numbers of atoms increase above some critical values N_B^c and N_F^c, an instability occurs [2]. It has been shown that the mean-field framework is able to reproduce the critical numbers for collapse [9]. We have calculated the stability diagram of the ^{40}K–^{87}Rb mixture by solving coupled mean-field Eqs. (5) and (6) for different values of N_B and N_F. In our study, the instability signature is the failure of the numerical iterative process. In particular, the instability onset appears as an indefinite growth of the maximum of the densities, which triggers the collapse.

We display in Fig. 3 the stability diagram for the ^{40}K–^{87}Rb mixture in the $N_B - N_F$ plane. The dots are the theoretical prediction for (N_B^c, N_F^c). The lines have been drawn to guide the eye and represent the critical instability lines that determine the boundary between

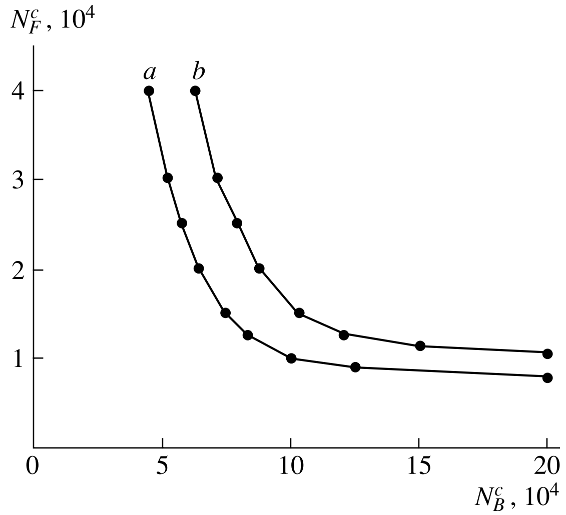

Fig. 3. Stability diagram of the ^{40}K–^{87}Rb mixture as a function of the number of atoms. The dots are the predictions for the critical number of bosons and fermions. The lines have been drawn to guide the eye and represent the critical instability lines that determine the boundary between the stable (left) and unstable (right) regions in two different cases: (*a*) a vortex free configurations and (*b*) bosons hosting a vortex line.

the stable (left) and unstable (right) regions in two different cases: (*a*) vortex-free configurations and (*b*) vortex state in the condensate component of the Fermi–Bose mixture. From Fig. 3 one can conclude that, for the ^{40}K–^{87}Rb mixture, the presence of a vortex in the condensate allows for a stable mixture for larger particle numbers. The reason is that a vortex state, as well as a sag displacement [22], diminishes with respect to the concentric case with no vorticity the enhancement of the density of both species in the overlap volume caused by their attractive mutual interaction.

4. SUMMARY

We have studied vortex states in Fermi–Bose mixtures with attractive mutual interactions. In particular, we studied ^{40}K–^{87}Rb mixtures confined in spherically symmetric trapping potentials for both species.

We have derived analytical formulas for estimating the position of the maximum of the fermionic and bosonic densities in two different limiting cases: (i) when $N_B \gg N_F$ and the condensate is in the Thomas–Fermi regime, and (ii) when the numbers of bosons and fermions are large. In both cases we obtained the same analytical expression: the position of the maximum of fermions is proportional to the position of the maximum of bosons by a factor that only depends on γ_r. This dimensionless parameter depends only on the values of the boson and boson–fermion scattering lengths, masses, and confining frequencies, and it yields that, in ^{40}K–^{87}Rb, the maxima of both species are very close.

We have solved numerically the coupled mean-field equations (GP equation for bosons coupled to the TFW equation for fermions) for different numbers of bosons and fermions. We have shown that the position of the maximum of the condensate density is fixed by the presence of a quantized vortex and that it is insensitive to the presence of trapped fermions. Moreover, we have seen that the position of the maximum of the fermionic density is also very insensitive to the fermion concentration N_F/N_B and that it is located close to the maximum of the condensate density. The analytical values are thus in good agreement with the numerical results and remain valid up to the critical atomic numbers.

Finally, we have shown that the critical atomic numbers that the mixture can sustain before it collapses may be increased when the condensate hosts a quantized vortex line. In this case, a larger overlap region between both species has been found, which may favor sympathetic cooling.

ACKNOWLEDGMENTS

This work has been performed under grant nos. BFM2002-01868 from DGI, Spain, and 2001SGR-00064 from Generalitat de Catalunya. D.M.J. has also been funded by the M.E.C.D. (Spain) on sabbatical leave. M.G. thanks the "Ramón y Cajal" Program of the Ministerio de Ciencia y Tecnología (Spain) for financial support.

REFERENCES

1. K. Molmer, Phys. Rev. Lett. **80**, 1804 (1998).
2. R. Roth, Phys. Rev. A **66**, 013614 (2002).
3. A. G. Truscott, K. E. Strecker, W. I. McAlexander, *et al.*, Science **291**, 2570 (2001).
4. F. Schreck, L. Khaykovich, K. L. Corwin, *et al.*, Phys. Rev. Lett. **87**, 080403 (2001).
5. Z. Akdeniz, P. Vignolo, A. Minguzzi, and M. P. Tosi, J. Phys. B **35**, L105 (2002).
6. G. Ferrari, M. Inguscio, W. Jastrzebski, *et al.*, Phys. Rev. Lett. **89**, 053202 (2002).
7. G. Modugno, G. Roati, F. Riboli, *et al.*, Science **297**, 2240 (2002).
8. G. Roati, F. Riboli, G. Modugno, and M. Inguscio, Phys. Rev. Lett. **89**, 150403 (2002).
9. M. Modugno, F. Ferlaino, F. Riboli, *et al.*, Phys. Rev. A **68**, 043626 (2003).
10. J. Goldwin, S. Inouye, M. L. Olsen, *et al.*, cond-mat/0405419 (2004).
11. L. Vichi, M. Amoruso, A. Minguzzi, *et al.*, Eur. Phys. J. D **11**, 335 (2000).
12. S. K. Yip, Phys. Rev. A **64**, 023609 (2001).
13. P. Capuzzi, A. Minguzzi, and M. P. Tosi, Phys. Rev. A **68**, 033605 (2003).

14. T.-L. Ho and V. B. Shenoy, Phys. Rev. Lett. **77**, 3276 (1996); D. M. Jezek, P. Capuzzi, and H. M. Cataldo, Phys. Rev. A **64**, 023605 (2001).
15. R. J. Donnelly, *Quantized Vortices in Helium II* (Cambridge Univ. Press, Cambridge, 1991).
16. M. R. Matthews, B. R. Anderson, P. C. Haljan, *et al.*, Phys. Rev. Lett. **83**, 2498 (1999).
17. A. L. Fetter and A. A. Svidzinsky, J. Phys.: Condens. Matter **13**, R135 (2001).
18. M. Guilleumas and R. Graham, Phys. Rev. A **64**, 033607 (2001).
19. C. J. Pethick and H. Smith, *Bose–Einstein Condensation in Dilute Gases* (Cambridge Univ. Press, Cambridge, 2002); L. Pitaevskii and S. Stringari, *Bose–Einstein Condensation* (Clarendon Press, Oxford, 2003).
20. R. Mayol, M. Pi, M. Barranco, and F. Dalfovo, Phys. Rev. Lett. **87**, 145301 (2001).
21. M. Barranco, M. Guilleumas, E. S. Hernández, *et al.*, Phys. Rev. B **68**, 024515 (2003).
22. D. M. Jezek, M. Barranco, M. Guilleumas, *et al.*, submitted to Phys. Rev. A (2004).